

The thermal expansion of carbon-fibre reinforced plastics

Part 6 *The influence of fibre weave in fabric reinforcement*

K. F. ROGERS, D. M. KINGSTON-LEE, L. N. PHILLIPS
Materials Department, Royal Aircraft Establishment, Farnborough, UK

B. YATES, M. CHANDRA*, S. F. H. PARKER
Department of Pure and Applied Physics, University of Salford, Salford, UK

The thermal expansion characteristics of a series of carbon-fibre fabric reinforced plastic laminates over the approximate temperature range 90 K to 440 K have been determined. The reinforcements included Morganite Type II fibres in a plain weave and a two-by-two twill weave and Courtaulds Grafil E/XAS fibres in a two-by-two twill weave, a five-shaft satin weave and in an unwoven unidirectional disposition. The results show that the ratio of fibre tow densities in the principal fibre directions, the crimp in the reinforcing fibres and the laminate stacking sequence all influence the magnitudes and temperature dependences of the linear thermal expansion coefficients, as well as the detailed manner in which the dimensions respond to changes of temperature. Volume shrinkage effects resulting from temperature cycling are also reported. The linear thermal expansion coefficients of Courtaulds Grafil E/XAS carbon fibres in directions parallel, α_{\parallel}^f , and perpendicular, α_{\perp}^f , to the fibre axis have been estimated as $\alpha_{\parallel}^f = -2.6 \times 10^{-7} \text{ K}^{-1}$ and $\alpha_{\perp}^f = 2.6 \times 10^{-5} \text{ K}^{-1}$.

1. Introduction

Earlier accounts [1-4] of the thermal expansion characteristics of carbon-fibre reinforced plastics have dealt with epoxy resin laminates reinforced with continuous, unwoven carbon fibres. However, carbon-fibre fabric reinforced plastics have found an increasingly wide range of applications in recent years because of the ability of the fabric to follow faithfully the contours of doubly-curved components. The present investigations have been undertaken in order to assess the influence of woven carbon fibres on the thermal expansion characteristics of the laminates they reinforce.

2. The specimens and their investigation

Table I contains a description of the specimens employed in the investigation. All specimens were based on the matrix resin DLS351/BF₃400, cured

by the cycle described earlier [2, 5], i.e., the resin was pre-cured on the fibre for 3 h at 100°C, the laminate pressed at 150°C for 2 h and then post-cured for 18 h at 190°C.

Plates 1 and 2 contained Morganite Type II carbon fibres[†]. Plates 3 to 6 contained Courtaulds Grafil E/XAS carbon fibres, XA denoting "Super A"-type fibre, S signifying that the fibres were surface-treated and E indicating that they were sized with uncured epoxy resin (Shell Epikote 834 in this case). Plate 1 contained 16 plies of plain-weave fabric woven from 5000-end carbon tows and laid up with the warp tows of each ply oriented in the same direction. Plate 2 contained 15 plies of 5000-end twill weave fabric similarly arranged. Plates 3 and 4 contained 25 plies respectively of twill weave and 5-shaft satin weave fabrics, similarly arranged but woven from thinner,

*Present address: Department of Electrical and Electronic Engineering, University of Bradford, Bradford, UK.

[†]High-strength fibres of a similar type to Courtaulds HTS fibres.

TABLE I The specimens

Plate number	Specimen designation	Fibre manufacturer	Fibre type	Weave	Direction of thermal expansion measurements	Fibre volume (%)	Void content (%)	Number of fibres per tow	Number of ends/picks per cm width
1	1	Morganite	Type II	Plain	Parallel to warp	60.1	3.0	5000	5.12
1	2	Morganite	Type II	Plain	Parallel to weft	60.1	3.0	5000	3.54
1	3	Morganite	Type II	Plain	Perpendicular to plane of laminate	60.1	3.0	5000	
2	4	Morganite	Type II	2 × 2 Twill (1)	Parallel to warp	61.1	3.6	5000	5.12
2	5	Morganite	Type II	2 × 2 Twill (1)	Parallel to weft	61.1	3.6	5000	3.90
2	6	Morganite	Type II	2 × 2 Twill (1)	Perpendicular to plane of laminate	61.1	3.6	5000	
3	7	Courtaulds	Grafil E/XAS	2 × 2 Twill (2)	Parallel to warp	60.0	0.5	3000	6.67
3	8	Courtaulds	Grafil E/XAS	2 × 2 Twill (2)	Parallel to weft	60.0	0.5	3000	6.18
3	9	Courtaulds	Grafil E/XAS	2 × 2 Twill (2)	Perpendicular to plane of laminate	60.0	0.5	3000	
4	10	Courtaulds	Grafil E/XAS	5 Shaft satin	Parallel to warp	59.1	2.2	3000	6.62
4	11	Courtaulds	Grafil E/XAS	5 Shaft satin	Parallel to weft	59.1	2.2	3000	6.12
4	12	Courtaulds	Grafil E/XAS	5 Shaft satin	Perpendicular to plane of laminate	59.1	2.2	3000	
5	13	Courtaulds	Grafil E/XAS	5 Shaft satin	Parallel to direction having 13 warps and 12 wefts	58.7	0.9	3000	
5	14	Courtaulds	Grafil E/XAS	5 Shaft satin	Parallel to direction having 12 warps and 13 wefts	58.7	0.9	3000	
6	15	Courtaulds	Grafil E/XAS	Unwoven (unidirectional)	Parallel to fibres	61.9	1.3	3000	
6	16	Courtaulds	Grafil E/XAS	Unwoven (unidirectional)	Perpendicular to fibres	61.9	1.3	3000	

3000-end, fibre tows. Plate 5 contained 25 plies of the 3000-end 5-shaft satin weave fabric laid up with the warp tows of the even-numbered plies at right-angles to the warp tows of the odd-numbered plies. Plate 6 contained unidirectional unwoven fibres abstracted from the 5-shaft satin fabric.

As well as noting that the scatter among the experimental in-plane results for the fabric-based laminates was generally larger than for laminates reinforced with unwoven fibres, it is reported later (Section 4.1) that unexpected differences were observed between the expansion behaviour in the warp and in the weft directions of laminates. In seeking causes of these phenomena, it was realized that 6.5 per cent of the weight of the fabrics consisted of resin size for which no allowance had been made in the amount of hardener added to the DLS 351, resulting in an incomplete cure of the final resin matrix in Plates 1 to 3. An appropriate addition for the resin size was made in the hardener used in Plates 4 to 6.

In the initial in-plane measurements on the fabric-reinforced laminates the test specimens were small rectangular parallelepipeds [1], and, to ensure their representative nature and their uniformity, their dimensions were chosen so that the pattern revealed in the surface layer was a representative unit of the overall pattern. After completing work on Specimens 6, the effect of specimen dimensions was investigated as a possible cause of the anomalous time-temperature behaviour mentioned above. In particular, the later specimens for in-plane observations were purposely prepared to dimensions as large as could be accommodated by the apparatus, taking the form of pairs of parallelepipeds clamped together with small brackets, this time conforming to two units of fabric pattern. Although no effects were detected from the change of shape and size, this larger specimen size was adopted in subsequent work.

Yet another attempt to determine the cause of the anomalous behaviour was made during the study of the specimens prepared from Plate 3. These were maintained under vacuum for several days in a desiccator prior to mounting in the test apparatus in order to remove moisture. All subsequent specimens were also subjected to this pre-treatment before test.

The thermal expansion determinations themselves were performed as described earlier [1], the specimens being mounted in sets of three as the

separators of the optically-flat plates of an interferometer. For the out-of-plane measurements single specimens only were used, each taking the form of a circular anchor ring of 20 mm inside diameter and of 28 mm outside diameter, of rectangular cross-section, the axis of which was perpendicular to the plane of the laminate from which it was cut and on the plane faces of which three small feet had been ground. Significant rotations of fringes were observed in the measurements conducted upon Specimen 6, but by adopting a procedure described elsewhere [6] a true average linear thermal expansion coefficient was obtained.

3. Results

Following previous practice, the results of the investigations are collected in smoothed numerical form for quantitative purposes in Table II. A graphical representation has been adopted for the primary data for comparative purposes (given in Figs 1 to 16). As mentioned in Section 2, it became apparent early in the work that the scatter of many of the in-plane experimental data was considerably higher than for the corresponding data for the laminates containing unwoven fibres. This led to the adoption of the alternative expansivity representation, $\Delta l/l$, the fractional length change resulting from an extensive change of temperature (l is the specimen length and Δl is the change in specimen length). The expansivity results for Specimens 1 to 16 are displayed in Figs 17 to 23. These are followed by graphs of the temperature-dependent changes of area of Plates 1 to 4, (Fig. 24). Figs 25 to 28 illustrate irreversible length changes accompanying the heating and cooling of the specimens.

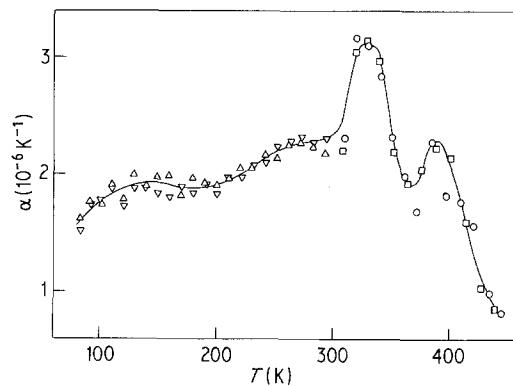


Figure 1 The linear thermal expansion coefficient, α , of Specimens 1: \circ Run 1; \square Run 2; \triangle Run 3; ∇ Run 4.

TABLE II Smoothed values of the linear thermal expansion coefficients, α , of the specimens described in Table I

T (K)	α (K ⁻¹) for the specimens numbered below															
	1	2	3	4	5	6	7	8	9	10	11	12	13	14	15	16
	($\times 10^{-6}$)	($\times 10^{-6}$)	($\times 10^{-6}$)	($\times 10^{-5}$)	($\times 10^{-6}$)	($\times 10^{-6}$)	($\times 10^{-6}$)	($\times 10^{-6}$)	($\times 10^{-5}$)	($\times 10^{-6}$)	($\times 10^{-6}$)	($\times 10^{-5}$)	($\times 10^{-6}$)	($\times 10^{-6}$)	($\times 10^{-6}$)	($\times 10^{-5}$)
90	1.68	2.71	1.61	1.48	2.35	1.77	1.61	1.65	1.82	2.10	2.11	1.93	2.22	2.20	0.38	1.49
100	1.77	2.73	1.71	1.48	2.35	1.87	1.62	1.68	1.93	2.15	2.14	2.03	2.22	2.22	0.37	1.57
120	1.89	2.81	1.91	1.49	2.37	2.07	1.64	1.74	2.15	2.22	2.20	2.26	2.24	2.25	0.33	1.73
140	1.96	2.90	2.11	1.50	2.39	2.27	1.67	1.80	2.35	2.26	2.26	2.46	2.26	2.28	0.28	1.87
160	1.92	3.00	2.29	1.52	2.43	2.44	1.70	1.86	2.55	2.29	2.32	2.65	2.29	2.32	0.24	2.03
180	1.89	3.11	2.48	1.54	2.47	2.62	1.74	1.93	2.75	2.32	2.37	2.85	2.34	2.36	0.21	2.18
200	1.92	3.25	2.65	1.56	2.53	2.78	1.78	2.00	2.95	2.37	2.41	3.03	2.40	2.42	0.18	2.33
220	2.00	3.41	2.81	1.60	2.61	2.93	1.84	2.08	3.14	2.45	2.47	3.18	2.49	2.49	0.16	2.49
240	2.13	3.62	2.97	1.69	2.69	3.07	1.88	2.17	3.33	2.58	2.60	3.35	2.62	2.57	0.17	2.64
260	2.23	3.90	3.11	1.84	2.80	3.19	1.98	2.26	3.50	2.77	2.80	3.52	2.77	2.68	0.20	2.79
280	2.28	4.24	3.24	2.07	2.92	3.40	2.07	2.37	3.69	2.95	3.00	3.69	2.95	2.84	0.25	2.94
300	2.35	4.18	3.46	2.44	3.06	3.77	2.17	2.49	3.90	2.70	3.08	3.81	3.02	3.00	0.31	3.10
320	3.05	3.54	3.92	2.85	3.23	3.92	2.29	2.66	4.15	2.62	3.02	3.89	2.89	2.93	0.37	3.25
340	2.93	3.45	4.00	3.16	3.44	3.96	2.40	2.89	4.42	2.85	2.87	3.92	2.71	2.72	0.43	3.41
360	1.99	4.16	4.16	3.38	3.67	4.20	2.52	3.17	4.68	3.08	2.91	3.98	2.72	2.72	0.49	3.56
380	2.19	4.48	4.53	3.55	3.96	4.60	2.62	3.30	5.03	3.27	3.49	4.18	3.45	3.28	0.53	3.75
400	2.07	4.42	4.96	3.66	4.23	5.03	2.72	3.32	5.42	3.41	4.10	4.79	3.97	3.79	0.47	3.97
420	1.32	3.90	5.37	3.72	4.33	(5.50)	2.80	3.24	6.03	3.50	4.03	5.91	4.12	3.96	0.34	4.23
440	0.87	2.47	5.76	3.66	3.86		2.87	2.94	7.15	3.37	3.55	7.42	3.95	3.89	0.14	4.56
450			5.94					2.58	8.25		2.96			(3.58)	(0.03)	

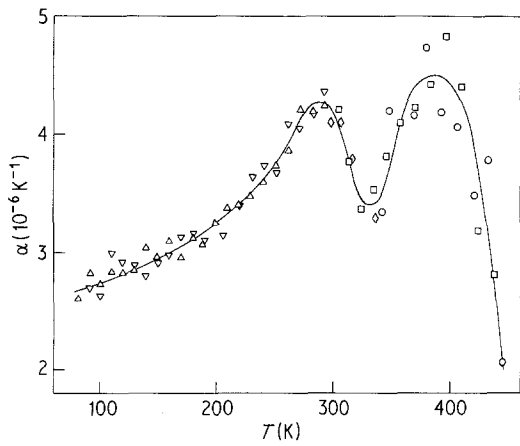


Figure 2 The linear thermal expansion coefficient, α , of Specimens 2: \circ Run 1; \square Run 2; \diamond Run 3; \triangle Run 4; ∇ Run 5.

4. Discussion

4.1. Comparative features

4.1.1. Plates 1 and 2

Plates 1 and 2 both contained Morganite Type II carbon fibre and for this reason a direct comparison of their thermal expansion characteristics is justified. The gross features of the in-plane results bear a resemblance to those seen in measurements conducted upon $0^\circ/90^\circ$ cross-plyed laminates laid up from unwoven fibres, e.g. Specimens 5 and 12 of [1]. However a fine

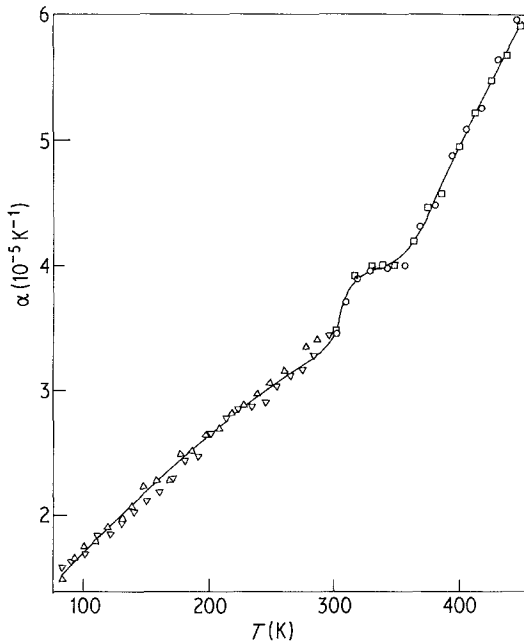


Figure 3 The linear thermal expansion coefficient, α , of Specimen 3: \circ Run 1, \square Run 2; \triangle Run 3; ∇ Run 4.

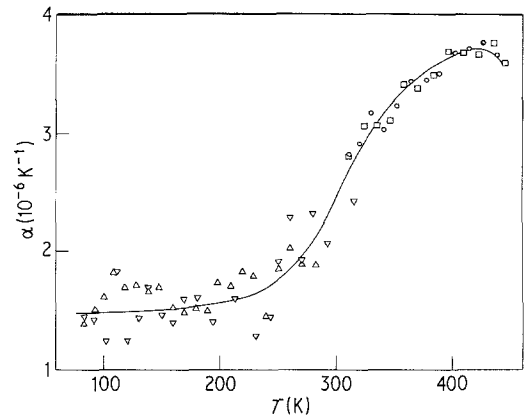


Figure 4 The linear thermal expansion coefficient, α , of Specimens 4: \circ Run 1; \square Run 2; \triangle Run 3; ∇ Run 4.

structure is discernible in the results for the laminate containing the plain weave, which contained the greatest degree of crimp of the four fabrics used in the programme. Comparing Fig. 1 with Fig. 2 and comparing Fig. 4 with Fig. 5, one may note that in both laminates the linear thermal expansion coefficient in the weft direction exceeds that in the warp direction. This difference is brought out in Figs 17 and 18, in which the corresponding expansivities are compared. The reason is presumably the differing numbers of tows in the two directions (Table I).

For the direction perpendicular to the plane, Figs 3 and 6 show that over the temperature range 290 K to 350 K there is a small hump, marking the position in temperature of a change in the curvature of the graphs. Corresponding features were

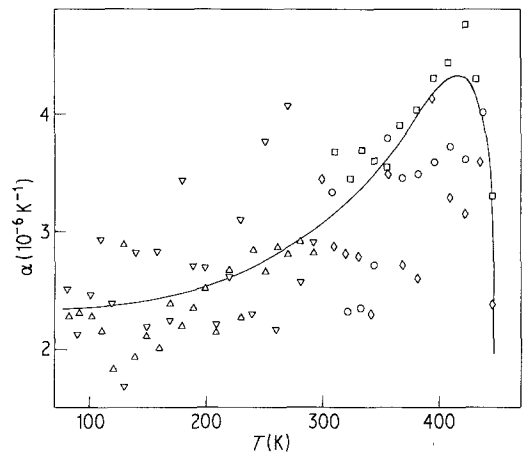


Figure 5 The linear thermal expansion coefficient, α , of Specimens 5: \circ Run 1; \square Run 2; \diamond Run 3; \triangle Run 4; ∇ Run 5.

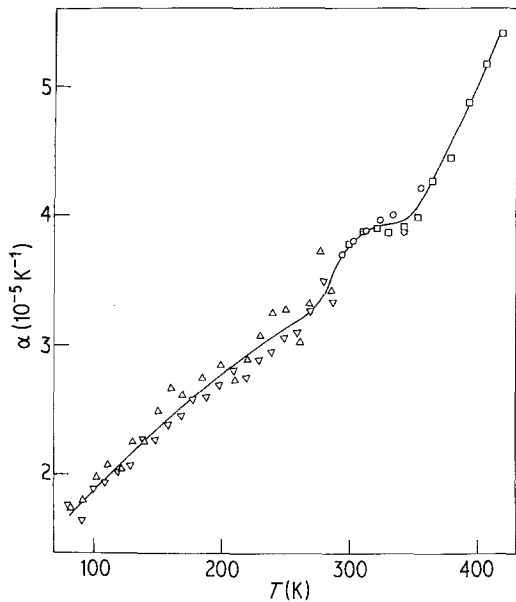


Figure 6 The linear thermal expansion coefficient, α , of Specimen 6: \circ Run 1; \square Run 2; \triangle Run 3; ∇ Run 4.

not obvious in the results for the direction perpendicular to the planes of any of the three 90° cross-plyed laminates containing unwoven fibres, for which results were reported in [1, 3]. The similarity of the out-of-plane expansivities of various 90° cross-plyes, illustrated in Fig. 21, shows how the behaviour of the resin predominates in this direction over any influence from the crimp in the fibres.

4.1.2. Plates 2 and 3

One advantage of employing commercially-available carbon-fibre cloth in these determinations is that the results obtained are of immediate technological value to the manufacturers of com-

ponents. A disadvantage is that in changing from one commercial material to another more than one factor is changed at a time, which makes it difficult to identify the precise cause of some of the resulting effects. Plates 2 and 3 illustrate this point. In particular, Table I shows that the parameters changed include fibre type, number of fibres per tow, number of ends/picks per unit width of fabric and ratio of fibre tow density in the warp to that in the weft.

A comparison of Figs 7 and 8 with Figs 4 and 5 reveals that here also the linear thermal expansion coefficient in the weft direction exceeded that in the warp direction. The cause presumably lies in the lower number of weft tows than warp tows in both laminates. Although the excessive scatter in the results for Specimens 5 limits the accuracy with which the temperature dependence of the linear thermal expansion coefficient may be discerned, the predominant influence of the weft fibres over the warp fibres of Plate 3 in causing the rapid fall at the higher temperatures is unambiguous. Because the fibre tow density in the weft direction is lower than in the warp direction, this predominance can only be due to the lesser crimp in the weft direction (a particular feature of rapier loom weaving), which permits the fibres to exert their influence in the manner observed in the fibre directions of $0^\circ/90^\circ$ laminates containing unwoven fibres, i.e., Specimens 5 (HTS* fibre) and 12 (HMS† fibre) of [1] and Specimens 28 and 33 of [3]. This aspect of the influence of crimp may be appreciated more clearly by referring to Figs 20 and 21 of [1], which illustrate the increasingly negative thermal expansion resulting from increasing the interply angle of bi-axially reinforced laminates from zero up to approximately 60° . It is

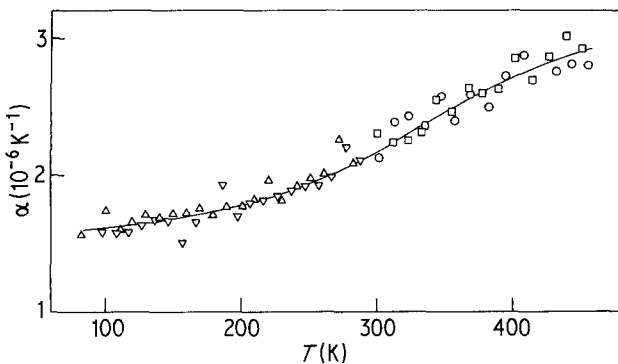


Figure 7 The linear thermal expansion coefficient, α , of Specimens 7: \circ Run 1; \square Run 2; \triangle Run 3; ∇ Run 4.

*Courtaulds high tensile strength surface-treated carbon fibre.

†Courtaulds high modulus surface-treated carbon fibre.

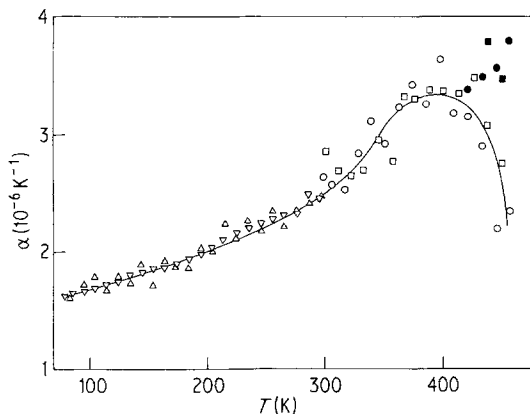


Figure 8 The linear thermal expansion coefficient, α , of Specimens 8: ● Run 1 (before equilibrium); ■ Run 2 (before equilibrium); ○ Run 1 (at equilibrium); □ Run 2 (at equilibrium); △ Run 3, ▽ Run 4.

apparent that the crimp each tow possesses is in the opposite sense to that of the adjacent tows. This implies that the laminate can be considered as an aggregate of minute angle-ply laminates, albeit aligned in the out-of-plane direction. Comparing Fig. 19 with Fig. 18, one may note that the closer similarity of the fibre tow densities in the warp and weft directions of Plate 3 compared with Plate 2 is reflected in a closer similarity between the corresponding expansivities.

Comparing linear thermal expansion coefficients perpendicular to the planes of Plates 2 and 3 (Figs 6 and 9), there is in Fig. 9 a noticeable absence of hump at a position in temperature at which the resin shows signs of dominating the behaviour of the composite, in contrast to that observed in the results for Specimens 3 and 6. One is led to con-

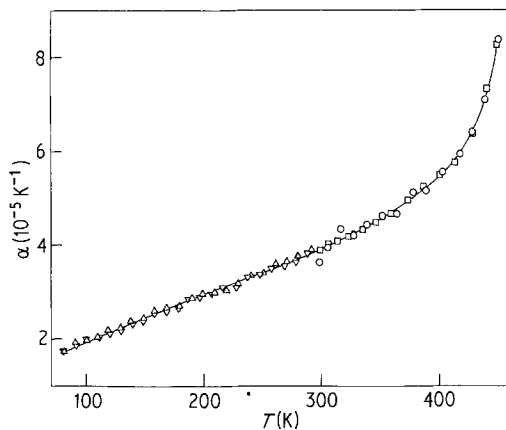


Figure 9 The linear thermal expansion coefficient, α , of Specimen 9: ○ Run 1; □ Run 2; △ Run 3; ▽ Run 4.

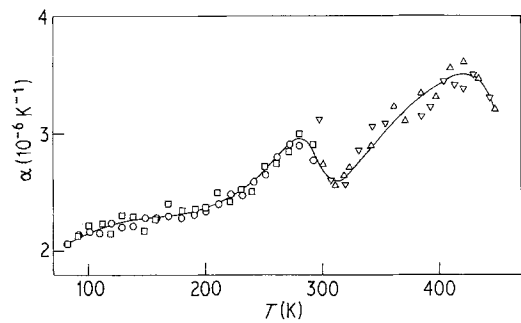


Figure 10 The linear thermal expansion coefficient, α , of Specimens 10: ○ Run 1; □ Run 2; △ Run 3; ▽ Run 4.

clude that this characteristic feature should be associated with Morganite Type II fibres. Comments appropriate to the influence of the resin in dominating thermal behaviour in a direction perpendicular to the plane of the laminate, (Fig. 21), resemble those made for Specimens 3 and 6.

4.1.3. Plates 3 and 4

One significant difference between Plates 3 and 4 is the structure of the reinforcing fabric: Plate 3 being two-by-two twill and Plate 4 being five-shaft satin. The difference between the linear thermal expansion coefficients in the warp and weft directions, (Figs 10 and 11), is much smaller than that observed for earlier laminates and this small difference becomes particularly noticeable when the expansivities are compared (Fig. 2). The crimp in the five-shaft satin weave is the least marked of the three weaves under investigation, and in consequence the resin in Plate 4 was subjected to greater in-plane stress than that of Plates 1 to 3. It

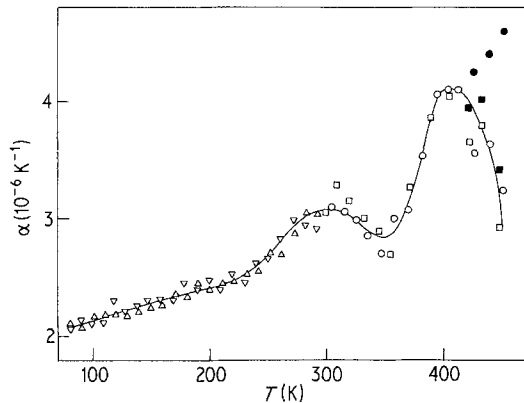


Figure 11 The linear thermal expansion coefficient, α , of Specimens 11: ● Run 1 (before equilibrium); ■ Run 2 (before equilibrium); ○ Run 1 (at equilibrium); □ Run 2 (at equilibrium); △ Run 3; ▽ Run 4.

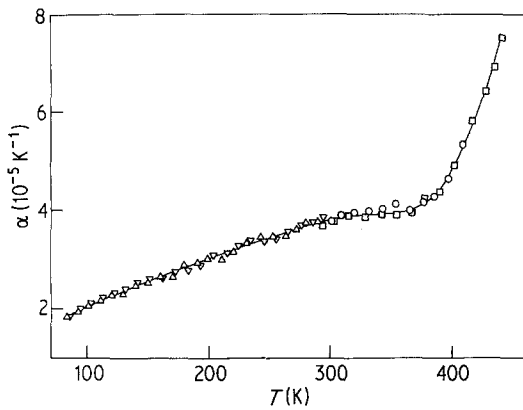


Figure 12 The linear thermal expansion coefficient, α , of Specimens 12: \circ Run 1; \square Run 2; \triangle Run 3; ∇ Run 4.

is therefore not surprising that the undulations observed in the results for Specimens 10 and 11 should resemble those in the results for Specimens 21 of [2], (resin DLS351/BF₃400 reinforced unidirectionally with HTS carbon fibre) and Specimens 33 of [3], (resin DLS351/BF₃400 reinforced with unwoven HTS carbon fibres cross-plyed at 0°/90°). The origin of these undulations is presumably the same as that of the effects observed at comparable temperatures in the differential calorimetric investigations conducted on the pure resin, as described earlier [2].

An association of a low-temperature anomaly in the viscosity of a resin with free volume effects [7] leads to the conjecture that "anomalies" in the thermal expansion characteristics of the composites in the present investigations may be in part attributable to free volume effects associated with the vibrations of cross-linked groups of atoms within the resin matrix and which show up when

the resin is in a stressed condition, rather than with effects involving molecular back-bone chains.

The results for the linear thermal expansion coefficient of Specimen 12 (Fig. 12) are very similar to those for Specimen 9 (Fig. 9) and those for Specimen 34 of [3]. The results for all three specimens indicate that in the direction perpendicular to the plane of a 0°/90° cross-ply, details of the in-plane weave are of secondary importance compared with the properties of the resin matrix. This point is brought out in Fig. 21, in which the corresponding out-of-plane expansivities may be seen to be very much alike.

4.1.4. Plates 4 and 5

Whereas in Plate 4 the warp tows of each layer were orientated in the same direction and the weft tows were orientated at 90° to them, in Plate 5 the warps and wefts were alternated intentionally, layer to layer. Predictably, any difference between the linear thermal expansion coefficients of Specimens 13 and 14 (Figs 13 and 14) is within the limit of experimental uncertainty. The results, as expected, are qualitatively similar to those for Specimens 10 and 11, especially the latter.

4.1.5. Plate 6

Experimental results for the linear thermal expansion coefficients parallel and perpendicular to the fibre direction of Plate 6 are shown in Figs 15 and 16. A comparison of these with the corresponding results for an earlier bar of the same resin reinforced unidirectionally with HTS carbon fibres, i.e., Specimens 21 and 22 of [2], reveals some unexpected points. The most obvious is that the transverse linear thermal expansion coefficient of Plate 6 exceeds that of specimens 22 of [2], sug-

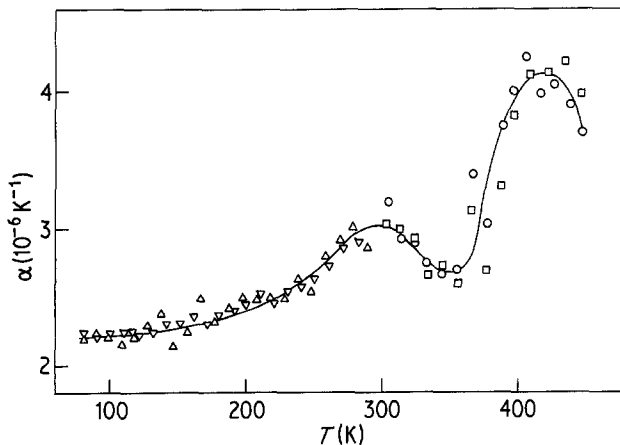


Figure 13 The linear thermal expansion coefficient, α , of Specimens 13: \circ Run 1; \square Run 2; \triangle Run 3; ∇ Run 4.

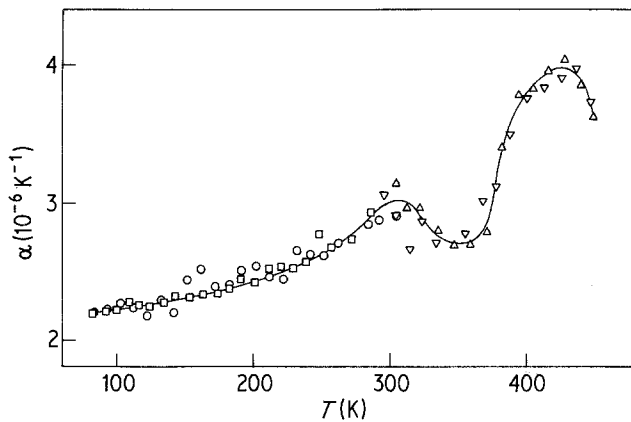


Figure 14 The linear thermal expansion coefficient, α , of Specimens 14; \circ Run 1; \square Run 2; \triangle Run 3; ∇ Run 4.

gesting that the c -axis of the graphite crystallites within E/XAS fibres may be more nearly at right-angles to the axis of the fibres than was the case with HTS fibres. Considering Fig. 15, the fact that the temperature at which the longitudinal linear thermal expansion coefficient of Plate 6 proceeds to fall with increasing temperature (approximately 380 K) is lower than that at which the corresponding fall occurs in the results for Specimens 21 of [2], (approximately 420 K), lends support to this view. On the other hand, the fact that the average value of the linear thermal expansion coefficient of Specimens 15 of this investigation exceeds that of Specimens 21 of [2] does not accord with a simple explanation of comparative features based upon a relative orientation of essentially similar crystallites.

The occurrence of a subsidiary maximum and minimum in the in-plane results for a DLS351/BF₃400 HTS 0°/90° cross-plyed laminate (Specimens 33 of [3]) was matched by a similar maximum and minimum in the results for the fibre direction of a DLS351/BF₃400 unidirectional HTS laminate (Specimens 21 of [2]). Attention has already been drawn to the similarity of these

features with those of the results for Specimens 10, 11, 13 and 14 of the present investigation and the effects have been attributed to internal changes within the resin. In retrospect, the fine structures of the results for Specimens 1 and 2 also bear a similarity to these features. By analogy, one might expect similar features in the results for the unidirectional Specimens 15, and their absence is puzzling. No less puzzling is the absence of an analogous fine structure in the results for Specimens 4, 5, 7 and 8. It seems improbable that the cause should lie in a variable moisture content, since the results are reproducible from one occasion to another. It is more likely to be the effect of variation in the resin constitution caused by unavoidable process variations during the curing cycle.

4.2. The influence of crimp

Attention has already been given to the difficulties in drawing conclusions from experimental results for laminates reinforced with carbon-fibre cloth, which are imposed by varying more than one structural parameter at a time. In identifying the effects of crimp it should be noted from Table I

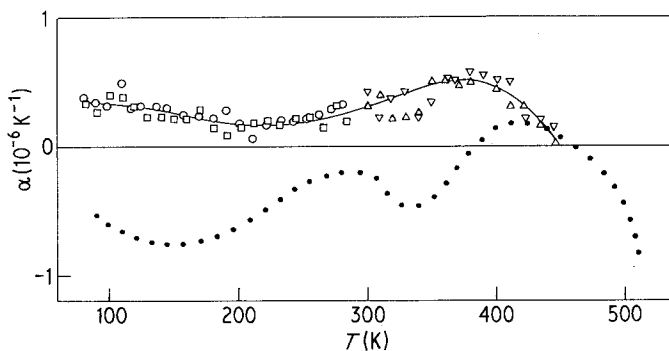


Figure 15 The linear thermal expansion coefficient, α , of Specimens 15: \circ Run 1; \square Run 2; \triangle Run 3; ∇ Run 4. The dotted line shows smoothed results for Specimens 21 of [2].

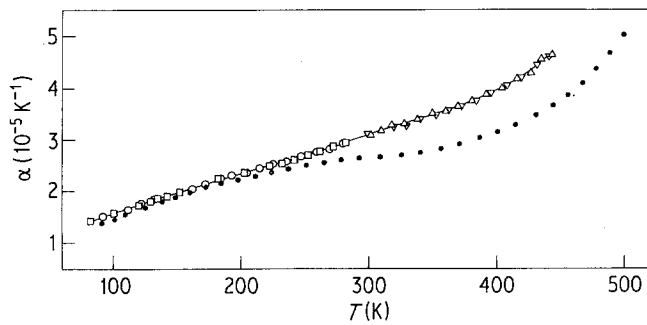


Figure 16 The linear thermal expansion coefficient, α , of Specimen 16: \circ Run 1; \square Run 2; \triangle Run 2; ∇ Run 4. The dotted line shows smoothed results for Specimens 22 of [2].

that the ratio:

$$\frac{\text{Number of fibres per unit width of warp direction}}{\text{Number of fibres per unit width of weft direction}},$$

henceforth denoted by N , diminishes from 1.45 for Plate 1, through Plates 2, 3 and 4 to unity in the case of the unidirectional HTS/DLS351 Bar 16 of [3]. This variation (shown in Table III), was taken into account when concluding earlier that the lesser crimp in the weft direction of Plate 3 compared with that in the warp direction resulted in the fall of the linear thermal expansion coefficient of Specimens 8 occurring at a lower temperature than was the case with Specimens 7, even though the average linear thermal expansion coefficient of Specimens 8 was greater than that of Specimens 7 because of the lower axial fibre density.

As an attempt to partially overcome differential effects associated with directionally different fibre tow densities, the temperature dependences of areas of plates have been expressed as fractions of their values at 100 K and compared in Fig. 24; 100 K was chosen since at this temperature there should be no complications due to debonding. The actual value of the ratio of an area, A_T , at temperature T , to its value at 100 K, was calculated

from the equation

$$\frac{A_T}{A_{100}} = 1 + \int_{100}^T (\alpha_{\text{warp}} + \alpha_{\text{weft}}) dT,$$

where α_{warp} and α_{weft} are the linear thermal expansion coefficients in the warp and weft directions of a plate, respectively. Bearing in mind the differences between the structures of the plates which are not removed by this form of representation one would be unwise to attach undue significance to small differences between the graphs. The safest conclusion is the obvious one, that the influence of weave upon the temperature dependence of the planar surface area of a laminate is of secondary importance compared with the massive decrease in the area thermal expansion of a resin matrix caused by the introduction of 90° cross-plyed fibre itself, irrespective of weave.

4.3. Temperature-dependent length change reversals

During the early stages of the investigation, when specimens prepared from Plate 1 were being investigated, it was observed that above a certain temperature the manner in which the length of specimens cut parallel to the weft direction

TABLE III Structural features of the plates

Plate/Bar number	Weave	Crimp	N (see text for definition)
1	Plain (Morganite Type II fibre)	Most marked	1.45
2	2 by 2 twill (Morganite Type II fibre)	Intermediate	1.31
3	2 by 2 twill (Courtaulds E/XAS fibre)	Intermediate	1.08
4	5 shaft satin (Courtaulds E/XAS fibre)	Least marked	1.08
16 of [3]	Unwoven $0^\circ/90^\circ$ cross-plyed fibres (Courtaulds HTS fibre)	None	1.00

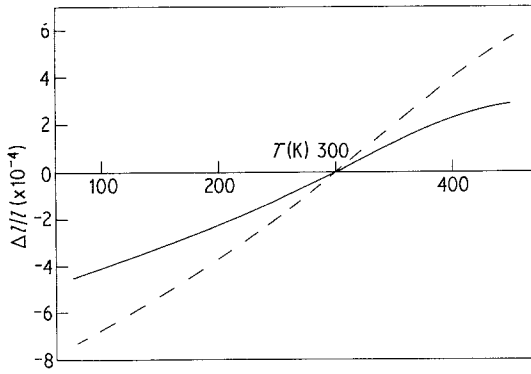


Figure 17 The (smoothed) linear thermal expansivities, $\Delta l/l$, of Specimens 1 and 2, referred to the length at 300 K. — warp direction; - - - weft direction.

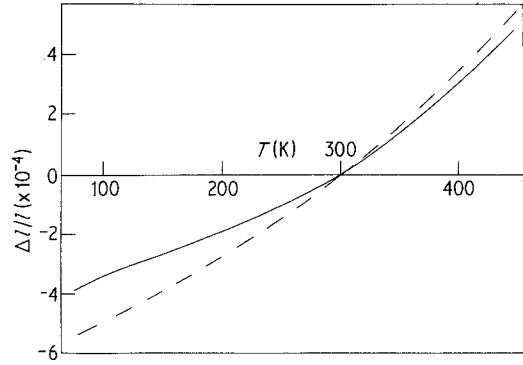


Figure 18 The (smoothed) linear thermal expansivities, $\Delta l/l$, of Specimens 4 and 5, referred to the length at 300 K. — warp direction; - - - weft direction.

responded to an increase of temperature of, typically, 10 K was different from that observed in the warp direction or in a direction perpendicular to the plane of the laminate. In particular, in the weft direction the specimens would first expand and then contract by anything up to 50% of the expansion before stabilizing. It was presumed, though not proved, that the magnitude of the difference between the behaviour in the warp and weft directions increased with the heating rate, starting from zero in the limiting case of an infinitely-slow temperature rise. Typical results of such observations are recorded in Figs 8 and 11. As explained in Section 2, the possible association of these effects with: (i) a deficiency of hardener in the matrix, (ii) specimen dimensions and (iii) a variable moisture content were eliminated systematically. The only in-plane specimens containing weft fibres which did not display these reversals were Specimens 13 and 14, in which the numbers of warps and wefts in the principal in-plane directions were approximately equal. Combining this observation with the absence of a reversal in the temperature-dependent dimensional behaviour within the plane of the

corresponding balanced laminate reinforced with 90° cross-plyed unwoven fibres, i.e., Specimens 33 of [3], one is left with two possible causes, either separate or in combination. These are:

- (i) the imbalance of fibre tow densities in the warp and weft directions;
- (ii) the different degrees of crimp in the warp and weft directions.

The question could be resolved by weaving a special cloth in which either the fibre tow densities in the principal fibre directions were arranged to be different while the crimps were arranged to be the same, or one in which the fibre tow densities were arranged to be the same and the crimps were arranged to be different. At the present time one can only conclude that temperature-dependent length-change reversals may be avoided by distributing the tow densities and crimps evenly between the two principal fibre directions.

4.4. The dimensional effects of temperature cycling

As experience of the temperature-dependent dimensional behaviour of the fabric-reinforced laminates grew, casual observations of certain

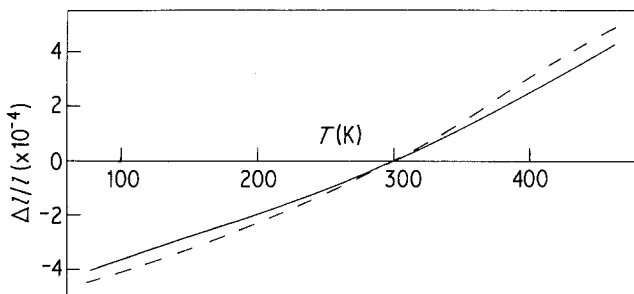


Figure 19 The (smoothed) linear thermal expansivities, $\Delta l/l$, of Specimens 7 and 8, referred to the length at 300 K. — warp direction; - - - weft direction.

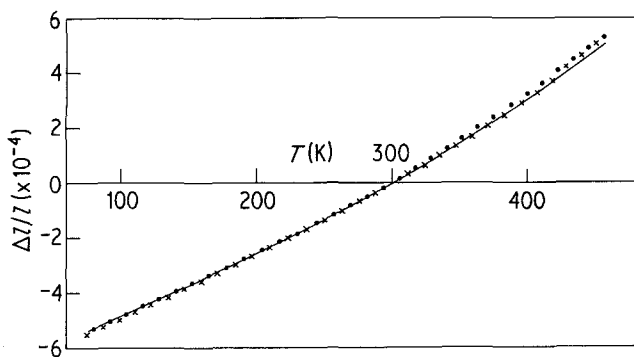


Figure 20 The (smoothed) in-plane linear thermal expansivities, $\Delta l/l$, of 90° cross-ply consisting of resin DLS351/BF₃400 containing nominally 60 vol% woven carbon fibres. — Specimens 10; ···· Specimens 11; x x x results for Specimens 13 and 14, not separable on this scale.

systematic effects for which explanations were not immediately obvious were recorded on a sufficient number of occasions to merit further investigation. In particular:

(i) The dimensional change corresponding to the first increase of temperature in a run was frequently well removed from the trend of the results which followed.

(ii) At the end of a sweep up and down an extended range of temperature above ambient, the number of fringes in the field of view was frequently different from the number at the outset.

(iii) Without actually counting the total number of fringes which passed the fiducial of the interferometer during sweeps of temperature above ambient, the observer had the impression that more fringes had passed on the return than on the outward run.

With a view to exploring total length changes resulting from rises or falls in specimen temperatures, attention was concentrated upon Plate 3. Fig. 25 shows the results of observations of integrated length increases in Specimens 7, which were

mounted in the high-temperature interferometer and heated at a steady rate of approximately 0.25 K min^{-1} . After reaching the highest temperature, the power supplied to the heater was reduced, allowing the assembly to cool at a rate approximately equal to the heating rate. As the temperature approached ambient temperature the cooling rate was very slow indeed and, because of this, observations were discontinued until the following day, when the procedure was repeated. Similar effects were observed with Specimens 8; examination of Fig. 26 shows that this time the range of temperatures covered in an excursion and the time allowed between excursions were varied deliberately. The heating rate in this and subsequent observations was maintained at 0.25 K min^{-1} . Summarizing the principal conclusions:

(a) In both warp and weft directions the final length is less than the original length.

(b) The length changes accompanying small temperature cycles (for example, 34 K) displayed qualitatively similar features to those accompanying large temperature cycles (for example,

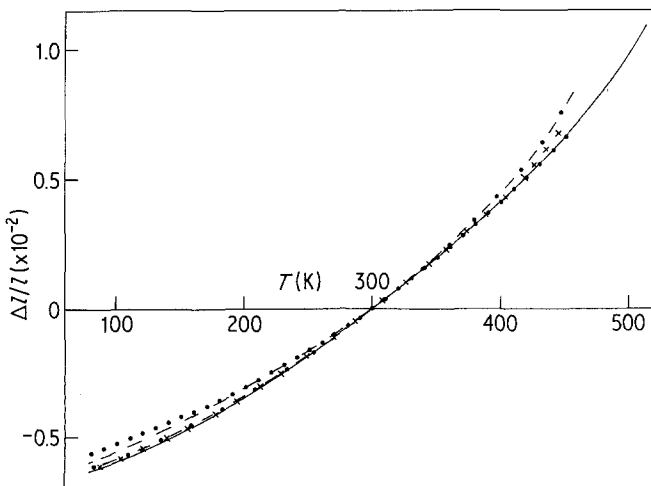


Figure 21 The (smoothed) out-of-plane linear thermal expansivities, $\Delta l/l$, of 90° cross-ply consisting of resin DLS351/BF₃400 containing nominally 60 vol% woven carbon fibres. ···· Specimen 3; --- Specimen 6; - · - Specimen 9; x x x Specimen 12; — Specimen 34 of [3].

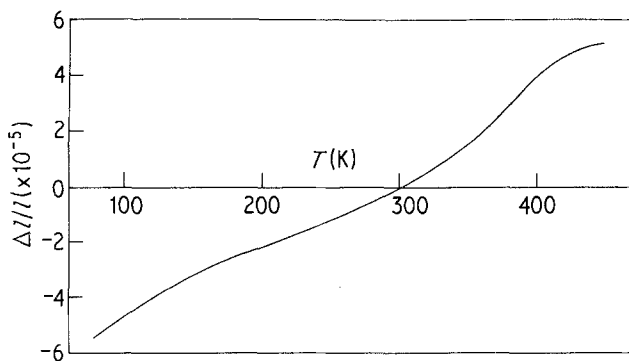


Figure 22 The (smoothed) linear thermal expansivity, $\Delta l/l$, of Specimens 15, referred to the length at 300 K.

156 K). Thus, the dimensional changes were not reversible for any increase of temperature covered, i.e., the effects did not correspond to elastic behaviour.

(c) The length change accompanying temperature cycling increased with the temperature range over which it was cycled.

(d) The length change resulting from cycling over a given temperature range was reduced by successive cycling.

(e) Displacements between outward and return runs were almost identical in the warp and weft directions. Thus, on the strength of the evidence available there is no reason to associate the irreversible temperature dependent length reductions with the reversals observed in the weft direction only.

Practical considerations did not permit the continuous monitoring of the dimensions of cycled specimens over extensive periods in a search for recovery affects. Instead, attention was directed to Specimen 9, which was cycled in a similar way over two successive days. The results of these measurements are displayed in Fig. 27. Comparing this with Figs 25 and 26, it is clear that the behaviours in each of the three principal directions of Plate 3 are essentially similar.

In order to establish whether or not these effects were peculiar to fabric reinforced laminates a return was made to Specimen 34 of [3], i.e., a specimen perpendicular to the plane of a DLS351/BF₃400 HTS 0°/90° cross plied laminate from unwoven fibre. The results of these measurements, shown in Fig. 28, are basically similar to the results shown in Fig. 27. It is reasonable to conclude from these observations that the contractions which result from temperature cycling do not depend on the weave or otherwise of the cross-ply. Indeed it seems likely that the effect is associated with the resin rather than with the fibres.

The elastic-plastic deformation induced by thermal stress in composites has been studied in some detail by Garmong [8] among others. An approach such as this, adapted to a comparable study of carbon fibre reinforced plastics in parallel with a study of the influence of absorbed moisture upon dimensions, might well elucidate the cause of the contractions resulting from temperature cycling.

4.5. The linear thermal expansion coefficients of Grafil E/XAS carbon fibres

It has been shown [2] that the application of theoretical models to experimental results for the

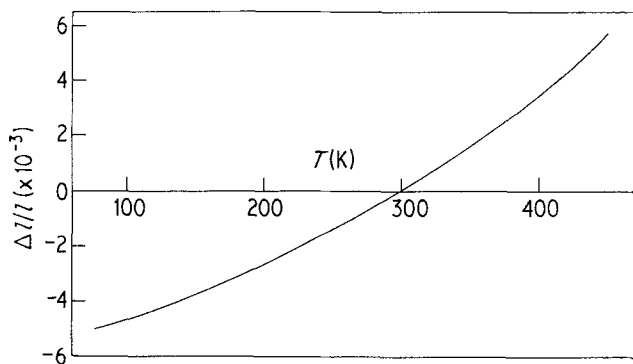


Figure 23 The (smoothed) linear thermal expansivity, $\Delta l/l$, of Specimens 16, referred to the length at 300 K.

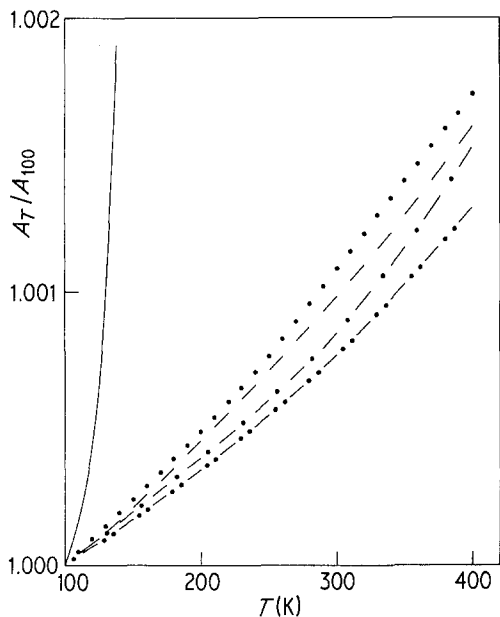


Figure 24 The temperature dependences of the areas of plates of DLS351/BF₃400 resin containing different reinforcements, expressed as fractions of the values at 100 K. — Specimens 18 of [2] (pure resin); ···· Plate 1; - · - Plate 2; - · · - Plate 3; - - - Plate 4.

linear thermal expansion coefficients of unidirectionally-reinforced carbon-fibre composite bars permits assessments to be made of the linear thermal expansion coefficients of the fibres in directions parallel and perpendicular to the fibre axis. The Young's moduli of the E/XAS fibres employed in the present investigation in directions parallel, E_{\parallel}^f , and perpendicular, E_{\perp}^f , to the fibre

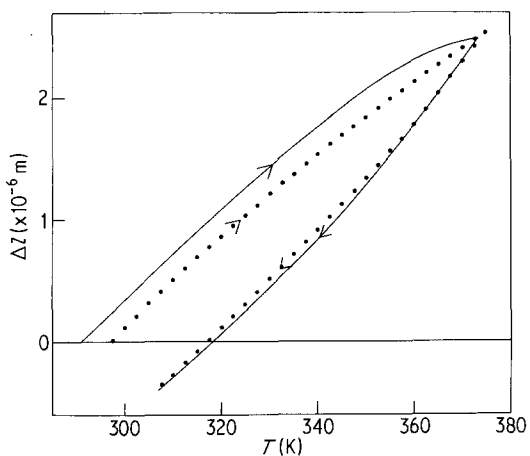


Figure 25 The temperature dependences of length changes, Δl , of Specimens 7, in which observations commenced at ambient temperature. — day 1; ···· day 2.

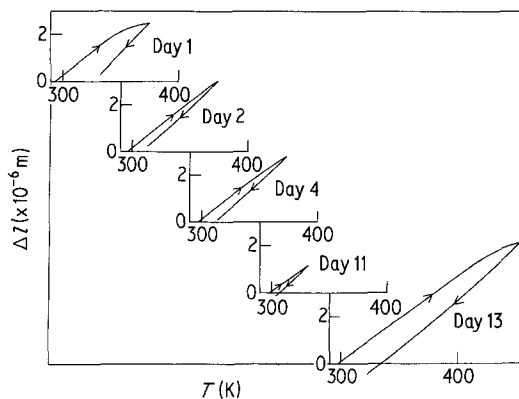


Figure 26 The temperature dependences of length changes, Δl , of Specimens 8, in which observations commenced at ambient temperature.

axis have been taken as $E_{\parallel}^f = 237 \text{ GN m}^{-2}$ and $E_{\perp}^f = 12.5 \text{ GN m}^{-2}$ (manufacturer's data). Employing these values and applying the procedure described earlier [2] to the results for Specimens 15 and 16 of this investigation and Specimens 18 of [2] (pure DLS351/BF₃400 cured resin), and in particular using the model of Chamberlain [9] for square packing, the linear thermal expansion coefficients of Courtauld's Grafil E/XAS fibres in directions parallel, α_{\parallel}^f , and perpendicular, α_{\perp}^f , to the fibre axis have been estimated to be:

$$\alpha_{\parallel}^f = -2.6 \times 10^{-7} \text{ K}^{-1}$$

and

$$\alpha_{\perp}^f = 2.6 \times 10^{-5} \text{ K}^{-1}.$$

Thermodynamic calculations of the isothermal

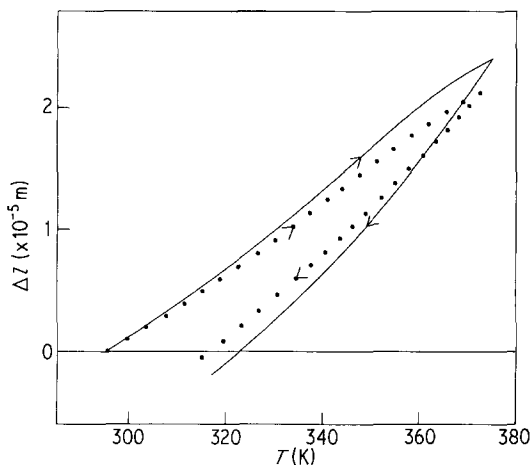


Figure 27 The temperature dependences of length changes, Δl , of Specimen 9, in which observations commenced at ambient temperature. — day 1; ···· day 2.

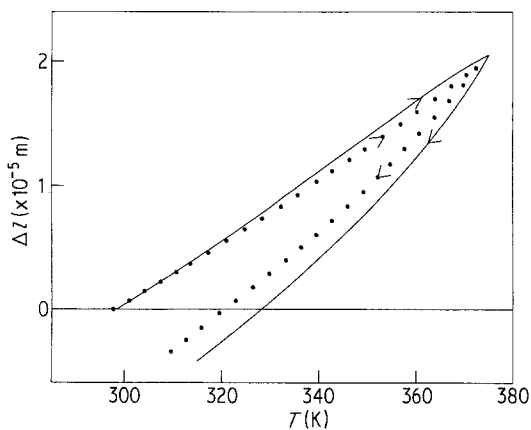


Figure 28 The temperature dependences of length changes, Δl , of Specimen 34 of [3], in which observations commenced at ambient temperature. — day 1; ··· day 2.

influence of pressure upon the volume thermal expansion coefficient of a solid, in terms of the isobaric temperature dependence of its isothermal bulk modulus of elasticity, indicated that the stress imposed upon the resin matrix by the included fibres was likely to reduce the volume thermal expansion coefficient of the resin. Lack of the appropriate data prevented the application of this correction during the course of the present calculations though, for temperatures reasonably below the resin glass transition temperature, T_g , its influence was not considered likely to be significant in comparison with the other uncertainties.

5. Appraisal and summary

At the outset of this investigation it was not anticipated that the thermal expansion characteristics of laminates reinforced with woven carbon fibres would differ significantly from those of laminates reinforced with unwoven fibres. As a broad generalization this is true, but the investigation has served to show how the relative orientation of constituent layers of fabric within a laminate can critically affect the manner in which its dimensions respond to changes of temperature. It has also been shown that alternation of orientation between layers leads to differences between the temperature-dependent length changes in the principal fibre directions which can be as much as 100%. By chance, and because standard commercially-available fabrics were used rather than specially prepared weaves, the ratio of the fibre tow densities in the principal fibre directions of the fabrics diminished with the crimp in the

fabrics containing them, which made tow density and crimp effects difficult to separate. However the balance of evidence available favours crimp as playing a significant rôle in controlling the temperature at which the influence of resin softening effects becomes apparent in the out-of-plane thermal expansion behaviour. It has also been shown that the fibre tow density undoubtedly plays a crucial rôle in governing the average values of the in-plane linear thermal expansion coefficients of a laminate.

Two points of general interest have emerged from the investigation. While seeking to establish the cause of the temperature-dependent length change reversals it was shown that, where the addition of approximately 13% less than the correct amount of hardener caused the resin to be incompletely cured, any effect on the thermal expansion behaviour was not obviously serious. Secondly, knowledge gained during the course of the investigation led to the conclusion that subjecting a $0^\circ/90^\circ$ laminate to temperature cycling resulted in a diminution of its volume: an effect which did not appear to be dependent upon the reinforcing fibres being woven. It was concluded that the effect was probably due to either residual thermal stresses or absorbed moisture.

Investigations such as this one inevitably leave a number of unanswered questions, and conclusions of a general nature contain the inherent danger of over-simplification. Until a detailed mathematical understanding of the thermoelastic behaviour of fibre-reinforced composites has been extended to cover the influence of crimp in fabric reinforcement, the scientific assessment of the significance of the present results must be limited to a qualitative appraisal. Technologically, one may conclude that differences between the temperature-dependent dimensional behaviour of laminates reinforced with woven fibres and those reinforced with unwoven fibres are not likely to cause problems in the majority of in-service applications, provided that proper attention is given to orientation and stacking sequence.

Acknowledgements

Mr Chandra wishes to record his gratitude to the Ministry of Defence for financial support. Dr Parker wishes to record his gratitude to the Science Research Council for financial support. This paper is published by permission of the Copyright © Controller, HMSO, London, 1981.

References

1. K. F. ROGERS, L. N. PHILLIPS, D. M. KINGSTON-LEE, B. YATES, M. J. OVERY, J. P. SARGENT and B. A. McCALLA, *J. Mater. Sci.* **12** (1977) 718.
2. B. YATES, M. J. OVERY, J. P. SARGENT, B. A. McCALLA, D. M. KINGSTON-LEE, L. N. PHILLIPS and K. F. ROGERS, *ibid* **13** (1978) 433.
3. B. YATES, B. A. McCALLA, J. P. SARGENT, K. F. ROGERS, L. N. PHILLIPS and D. M. KINGSTON-LEE, *ibid.* **13** (1978) 2217.
4. B. YATES, B. A. McCALLA, J. P. SARGENT, K. F. ROGERS, D. M. KINGSTON-LEE and L. N. PHILLIPS, *ibid.* **13** (1978) 2226.
5. B. YATES, B. A. McCALLA, L. N. PHILLIPS, D. M. KINGSTON-LEE and K. F. ROGERS, *ibid.* **14** (1979) 1207.
6. J. P. SARGENT and B. YATES, *Applied Optics* **17** (1978) 682.
7. D. H. DROSTE and A. T. DIBENEDETTO, *J. Appl. Polymer Sci.* **13** (1969) 2149.
8. G. GARMONG, *Metallurgical Transactions* **5** (1974) 2191.
9. N. J. CHAMBERLAIN, British Aircraft Corporation Report Number SON(P)33, (1968).

Received 16 February and accepted 26 March 1981.